# Nature of Latent Images Formed on Single Layer Organic Photoconductors

*Inan Chen*
*Quality Engineering Associates, Inc.*
*755 Middlesex Turnpike, Unit 3, Billerica MA 01821*
*Tel: 978-528-2034 · Fax: 978-528-2033*
*e-mail: info@qea.com*
*URL: www.qea.com*

# Nature of Latent Images Formed on Single Layer Organic Photoreceptors

*Inan Chen*
*Quality Engineering Associates (QEA), Inc., Burlington, Massachusetts*

## Abstract

The photoinduced discharge of single-layer organic photo-conductors involves photogeneration in the bulk, transport requirements for both holes and electrons, and bimolecular recombination during transit. In this paper, the impacts of these features on the formation of latent solid-area and one-pixel line images with laser exposure are mathema-tically analyzed. The results are compared with the case of images formed on dual-layer organic photoreceptors. A new insight into the advantage regarding image resolution is discussed.

## Introduction

In the application as electrophotographic photoreceptors, single-layer organic photoconductors (OPC) made by dis-persing pigments and charge-transport molecules in poly-mers are known to have many advantages over the more commonly used dual-layer OPC.[1,2,3] The obvious advantages include the simplicity of fabrication and the feasibility of (low ozone) positive corona charging. Another advantage, namely, a better image resolution, especially with laser (digital) exposure has been mentioned. On the other hand, photoinduced discharge in single-layer OPC involves com-plications arising from photogeneration of charge carriers in the bulk, transport requirements for both holes and electrons, and bimolecular recombination of holes and electrons during transit.

A previous analysis of photoinduced discharge with bulk photogeneration was carried out before digital electrophotography (EP) became popular.[4] There was little interest in the effects of bimolecular recombination arising from the high intensity short pulse of laser exposure, or the sharpness of pixel size images from laser beams with Gaussian profiles.

In this paper, these issues are considered in a mathematical analysis of latent image formation using single-layer OPC. The photoinduced discharge curves (PIDC), i.e., surface voltage vs. exposure curves, for solid-area images are analyzed first. Then, the surface voltage profiles of one-pixel line images are examined. The results are compared with the corresponding images formed on the traditional dual-layer OPC, and those formed with low intensity long duration (analogue) exposure. A new insight into the advantage regarding image resolution is discussed.
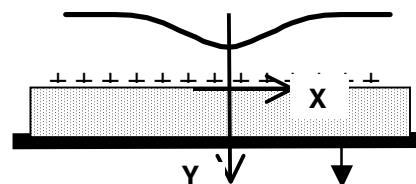


*Figure 1. Schematic of latent image formation on a surface-charged photoreceptor*

## Photogeneration and Charge Transport Equations

Consider a layer of OPC with a surface charge density $Q_s$ and a grounded substrate, as shown in Fig. 1. A line image is created by scanning a Gaussian laser beam along the z axis (perpendicular to the plane of figure). The transport of holes and electrons photogenerated in the OPC is described by the continuity equations for the hole- and electron-charge densities, $q_p(x, y, t)$ and $q_n(x, y, t)$,

$$\partial q_p/\partial t = -\text{div}(\mathbf{J_p}) + G + R, \text{ with } \mathbf{J_p} = \mu_p q_p \mathbf{E} \qquad (1a)$$

$$\partial q_n/\partial t = \text{div}(\mathbf{J_n}) - G + R, \text{ with } \mathbf{J_n} = \mu_n q_n \mathbf{E} \qquad (1b)$$

where $\mu_p$ and $\mu_n$ are the hole and electron mobility, respectively, and G and R represent the contribution from photogeneration and the loss due to bimolecular recom-bination of charges, respectively. Assuming the recombin-ation to follow the Langevin model, R can be expressed as,[5,6,7]

$$R(x, y, t) = (\mu_p - \mu_n)q_p q_n/\varepsilon \qquad (2)$$

where $\varepsilon$ is the permittivity of the OPC. Denoting the elemental charge by e, the photogeneration efficiency by $\eta$, the absorption coefficient of the incident light by $\alpha$, the light intensity at the beam center by $\phi_0(t)$, and the $1/e^2$ width of the Gaussian beam by s, the photogeneration term G can be expressed as,

$$G(x, y, t) = e\eta\alpha\phi_0\exp[-2(2x/s)^2]\exp(-\alpha y) \qquad (3)$$

The efficiency $\eta$ is in general field dependent. In digital EP, however, the laser exposure time $t_x$ for each pixel, being of the order of nano-sec, is negligibly short compared to the transit time ($t_T \approx 10$ msec) required for a hole or an electron

(with a mobility $\approx 10^{-6}$ cm$^2$/Vsec or less) to move across the OPC layer (of thickness $L \approx 20$ μm) under the typical electric field ($\approx 10^5$ V/cm) of interest in EP. Thus, all changes can be regarded as generated at the initial field $E_0 = V_0/L$ with the same efficiency η. In some OPC, the efficiency can also be intensity dependent. This would make the low intensity exposures less efficient than the high intensity exposures, and lead the PIDC to have the so-called "incubation" period, or "high gamma" feature. However, for lack of quantitative information (in particular, at digital exposure intensities), the efficiency is assumed to be intensity independent in this analysis.

The absorption coefficient α is related to the transmission optical density OD of a layer of thickness L by, OD = log[exp(αL)] = 0.4343αL, or αL = 2.3OD. The OD of typical single layer OPC is about OD $\approx 2$.[2]

Taking the end of digital exposure as $t = 0$, the initial distributions of holes and electrons can be written as,

$$q_p(x, y, 0) = -q_n(x, y, 0) = \alpha G_0 \exp[-2(2x/s)^2]\exp(-\alpha y) \quad (4)$$

where $G_0$ represents the charge generated during the exposure, at the line center,

$$G_0 = e\eta\phi_0 t_x \quad (5)$$

The electric field $\mathbf{E}(x, y, t)$ in Eq.(1) is related to the voltage $V(x, y, t)$ and the charge densities by the Poisson equation,

$$\text{div } \mathbf{E} = -\text{div}(\mathbf{grad}\ V) = (q_p + q_n)/\varepsilon \quad (6)$$

Typically, the charge mobility in such OPC is field dependent, and can be approximated by a power law,

$$\mu(E) = \mu_0(E/E_0)^m \quad (7)$$

where $\mu_0$ is the mobility at a field $E_0$, and m is a constant power. The surface charge density $Q_s(x, t)$ varies with time according to,

$$\partial Q_s/\partial t = -J_{py}(x, 0, t) - J_{ny}(x, 0, t)$$
$$= -[\mu_p q_p + \mu_n q_n]E_y(x, 0, t) \quad (8)$$

where $J_{py}$ and $J_{ny}$ are the y components of hole and electron conduction currents, respectively. The initial value of $Q_s$ is independent of x, and related to the initial surface voltage $V_0$ by $Q_s(x, 0) = Q_0 = CV_0$, where C is the capacitance of the photoreceptor. $Q_s$ is also related to the y component of the field $E_y$ by the Gauss theorem,

$$Q_s(x, t) = \varepsilon E_y(x, 0, t) \quad (9)$$

The above set of equations can be solved numerically for the calculations of surface charge $Q_s(x, t)$ or voltage

$V(x, 0, t)$ distributions at any later time. Examples of numerical results for solid-area images and line images are presented and discussed in the following sections.

## Solid-Area Images

For solid-area images, the equations are reduced to one-dimensional in space (the x-dependence eliminated). Examples of calculated time dependence of surface voltages for the case of OD = 2 (i.e., αL = 4.6) are shown in Fig. 2. The voltage is given in units of the (positive) initial surface voltage $V_0$, and the time is in units of the nominal transit time, $t_T = L^2/\mu_0 V_0$. The electron mobility is assumed to be 1/10 in magnitude of the hole mobility, $|\mu_n/\mu_p| = 0.1$, and both mobilities are linearly dependent on the field (m = 1 in Eq. 7). The exposure $\phi_0 t_x$ is varied in different curves, and represented by the values of $G_0$ (Eq. 5) in units of the initial surface charge density $Q_0$. It can be seen that the discharge is practically terminated after about $10t_T$ (typically $\approx$ 0.1 sec), and is hardly complete even with an exposure as large as $G_0 = 5Q_0$.
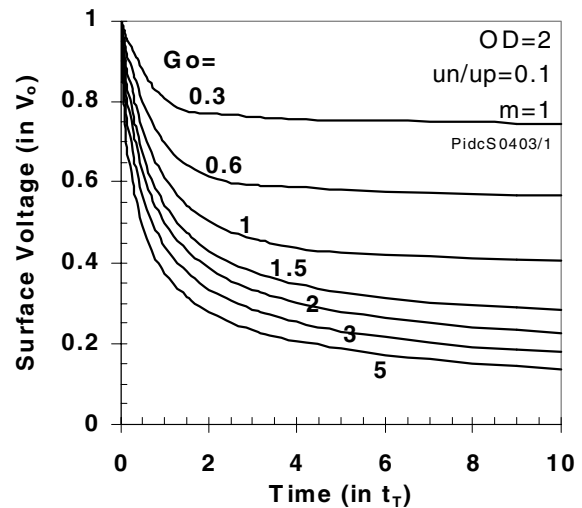


*Figure 2. Surface voltage decay calculated for different amounts of short pulse exposure, represented by $G_o$ in units of $Q_o$, in single-layer OPC with OD=2.*

The surface voltages at $t = 20t_T$ are shown as functions of exposure (i.e., PIDC) in Fig. 3. The four solid curves are calculated for the case of OD = 2, with different ratios of electron to hole mobilities, $|\mu_n/\mu_p|$, ranging from 1 to 0. Two dashed curves are added in Fig. 3 for comparison. The lower one represents the asymptotic solution, $V(G_0) = V_0\exp(-G_0/Q_0)$, obtained for spatially uniform photo-generation of charge and at $t\rightarrow\infty$.[7] With $|\mu_n/\mu_p| = 1$ and field-independent mobility, the PIDC (numerically) calculated at $t \geq 10t_T$ coincides well with the asymptotic PIDC. The upper dashed curve is the PIDC calculated for dual-layer OPC with photogeneration in a thin charge generation layer (CGL). At the same exposure, the voltage in this case is

generally higher than that in the asymptotic curve. This can be partially attributed to the larger recombination loss of photogenerated charge due to the higher charge density in the thin CGL. At higher exposures, the discharge is further reduced by the more severe space-charge effect due to monopolar (holes only) transport in the charge transport layer (CTL).[8,9]
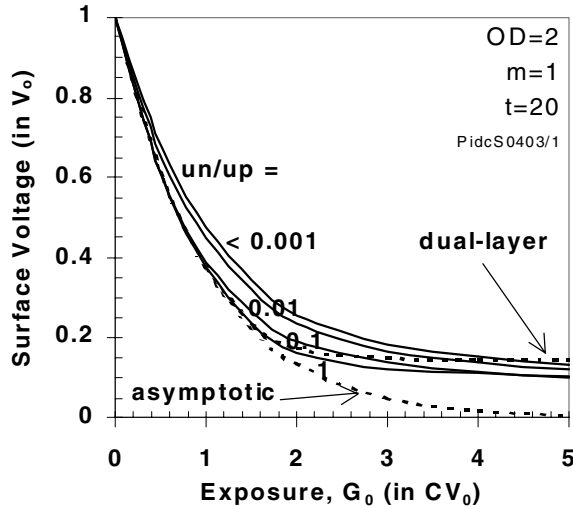


*Figure 3. Calculated PIDC of single-layer OPC with OD=2, and various mobility ratios $|\mu_n/\mu_p|$. The dashed curves are the PIDC for a dual-layer OPC and the asymptotic PIDC for uniform photogeneration.*

A somewhat unexpected result in Fig. 3 is the weak effect of the electron to hole mobility ratio, $|\mu_n/\mu_p| < 1$. Between the cases of $|\mu_n/\mu_p| = 1$ and $|\mu_n/\mu_p| = 0$, the residual voltages at an exposure of $5Q_0$ differ only 4% of $V_0$, (0.10 vs. $0.14V_0$). This weak effect of poor electron transport can be attributed to the "scavenging" by the larger number of holes generated in the front part of the layer, recombining with the smaller number of slower electrons generated in the rear as the holes move toward the substrate. This explanation is supported by the observation that the difference in surface voltages between the two cases ($|\mu_n/\mu_p| = 1$ and 0) is the largest ($\approx 11\%$ of $V_0$) at a smaller exposure, $G_0 \approx 1.5Q_0$, where the smaller densities of holes and electrons make the scavenging by recombination less efficient. Another support for this explanation is that a much stronger effect is seen if the hole mobility is the smaller one, i.e., $|\mu_p/\mu_n| < 1$, (in positively charged OPC), as shown in Fig. 4. In this case, there are not enough faster electrons (from the rear) moving toward the surface to recombine with (or scavenge) the larger number of slower holes generated in the front.

The total amount of charge recombined $Q_R$ is independent of the mobility ratio, and is equal to that in the asymptotic case, $Q_R = G_0 - Q_0[1 - \exp(-G_0/Q_0)]$.[7] Therefore, the higher voltages associated with lower $|\mu_n/\mu_p|$ in Fig. 3 (or lower $|\mu_p/\mu_n|$ in Fig. 4) are due to the slower electrons (or

holes) remaining in the bulk, and not due to smaller amount of effective (transit) charges.
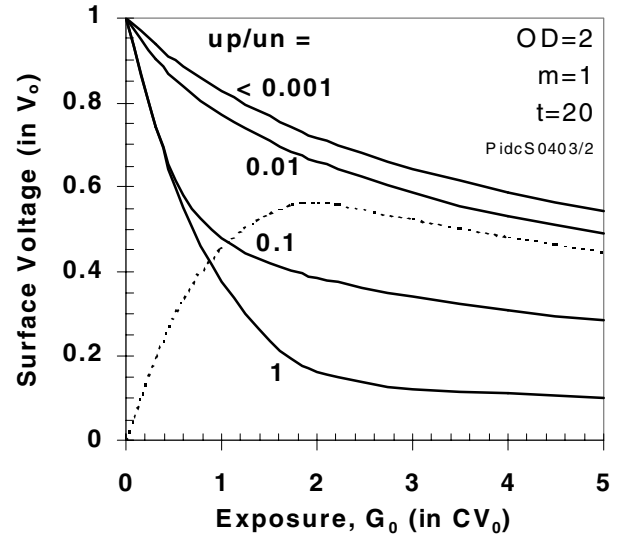


*Figure 4. PIDC calculated for the case of hole mobility smaller than electron mobility. The difference between voltages for $|\mu_p/\mu_n| = 1$ and 0 is shown by the dashed curve.*

While the exposure in digital EP is short and high in intensity as considered in the above examples, most reported PIDC measurements in laboratories to this date are carried out under the low intensity long time exposure conditions (as in analog EP). In the latter case, the photogeneration continues as the field decreases, and the efficiency η may decrease with time because of its field dependence. This is compensated by the smaller recombination loss due to lower charge densities during the discharge. Thus, the digital and analog types of PIDC may appear comparable. However, the low intensity and low charge density of analog type exposure also reduce the efficiency of scavenging the slower moving electrons by recombination. Therefore, the effect of mobility difference on the discharge can be more pronounced in PIDC measured with low intensity long duration (analog) exposure.

## One Pixel Gaussian Line Images

Examples of calculated surface voltage profiles (the latent images) resulting from one-pixel line exposure on single-layer OPC with OD = 2 are shown in Fig. 5. The $1/e^2$ width of the Gaussian beam is s = 2L, and the exposure time is $t_x \ll t_T$. The mobility ratio is $|\mu_n/\mu_p| = 0.1$, and the field dependence for both μ is linear (m = 1). The curves show the surface voltages at $t = 20t_T$ when the discharge is essentially terminated. The amount of exposure at the line center, represented by $G_0$ (Eq. 5) in units of $Q_0$, is varied.
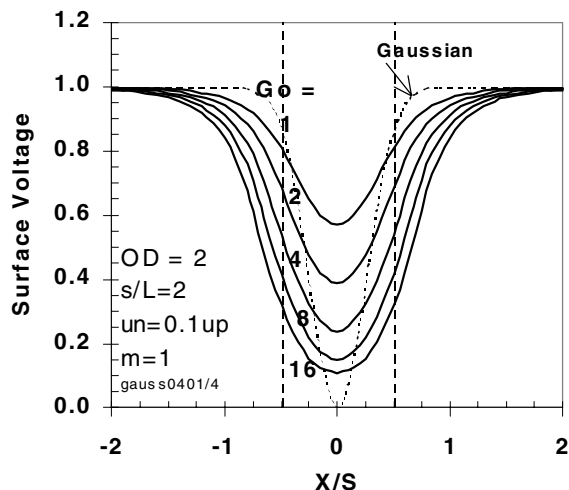
*Figure 5. Latent images (surface voltage profiles) of one pixel Gaussian line formed on single-layer OPC with OD=2, calculated for various exposure levels $G_o$.*
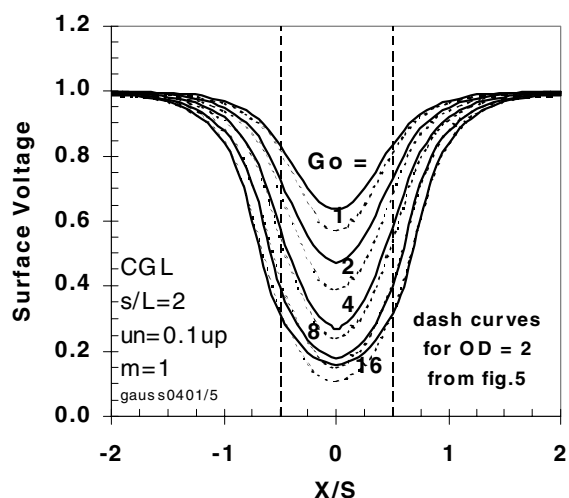


*Figure 6. Latent images of one-pixel Gaussian line formed on dual-layer OPC, calculated for various exposure levels $G_o$. The dashed curves are from Fig. 5.*

Comparing the voltages at the line center (x/s = 0) with those in solid-area images (Fig. 3), one sees that for the same exposure $G_0$, the discharge is much less in the line images. This can be attributed to the significant broadening of the latent images compared to the Gaussian exposure profile (dashed curve in Fig. 5).

The corresponding latent images formed on dual-layer OPC (with photogeneration in a thin CGL) are shown in Fig. 6. For comparison, the curves shown in Fig. 5 are superimposed as dashed curves. It can be seen that, contrary to common expectation, there is no significant difference in the line width or shape between the images from single-layer and dual-layer OPC. However, between the two sets of images (solid and dashed curves) there are slight differences

in the voltage depth at the line center (i.e., the contrast), in particular at an exposure of about $G_0 = 1\sim 2Q_0$. This larger contrast in single layer OPC can be attributed to smaller recombination and weaker space-charge effect due to bipolar transport (as also seen in solid area images of Fig. 3).

This means that, if the image resolution from single-layer OPC is really better than that from dual-layer OPC, the reason cannot be in the line width. The larger contrasts could be a factor, but others such as the intensity dependent photogeneration that leads to high gamma feature, mentioned in Introduction, should be an important factor.

## Summary and Conclusions

The nature of latent images formed on single-layer OPC with high intensity short pulse exposure of digital electrophotography is analyzed mathematically. From the investigations of solid-area images, it is shown that the deleterious effect of smaller electron mobility (with positive surface charge) is weaker than that observed in low intensity long duration (analog type) exposure. This is attributed to the scavenging of the slower electrons by recombination with the large number of faster holes.

For one-pixel line images, the line widths and shapes are found to be comparable to the corresponding images formed on dual-layer OPC. However, the image contrast, represented by the voltage depth at the line center, is found to be slightly larger in single layer OPC. This can be attributed to the smaller recombination loss when the charges are generated over a larger thickness. Additionally, the bipolar nature of space charges in single-layer OPC can reduce the space-charge limitation effect on charge transport associated with high charge density.

Although the numerical examples shown are for a special set of parameter values, similar features are seen and the same conclusions are drawn from calculations with other values of parameters within the range of practical interest.

## References

1. K. Kubo, T. Kobayashi, S. Nagae, and T. Fujimoto, Photoconduction mechanism in single layer photoconductor with metal-free phthalocyanine, *J. Imaging. Sci. Technol.* **43**, 248 (1999)
2. T. Nakazawa, On the materials design and photoconduction mechanism in positively charged single-layer organic photoconductors, *Doctoral thesis, Osaka University* (1994) (in Japanese)
3. Y. Mizuta, N. Akiba, Y. Watanabe, F. Sugai, S. Matsumoto, H. Nakamori, E. Miyamoto, and T. Nakazawa, Synthesis and xerographic properties of novel naphthoquinone, *Proc. IS&T's NIP13*, p. 197 (1997)
4. C. C. Kao and I. Chen, Xerographic discharge characteristics of photoreceptors with bulk generation I and II, *J. Appl. Phys.* **44**, 2708 and 2718 (1973)

5.   W. May, E. I. P. Walker, and D. C. Hoesterey, Bimolecular recombination in aggregate organic photoconductors, *J. Appl. Phys.* **50**, 8090 (1979)

6.   R. C. Hughes, Bulk recombination of charge carriers in polymer films: poly-N-vinylcarbazole complexed with trinitrofluorenone, *J. Chem. Phys.* **58**, 2212, (1973)

7.   I. Chen, Effects of bimolecular recombination on photocurrent and photoinduced discharge, *J. Appl. Phys.* **49**, 1162 (1978)

8.   I. Chen, Xerographic discharge characteristics of photoreceptors II, *J. Appl. Phys.* **43**, 1137 (1972)

9.   J. Mort and I. Chen, Physics of xerographic photoreceptors, *Applied Solid State Science*, vol. 5, p. 69 (R. Wolfe ed. Academic Press, New York, 1975)

## Biography

Inan Chen received his Ph.D. from the University of Michigan in 1964, and worked at the Research Laboratories of Xerox Corp. in Webster, New York from 1965 to 1998. Currently, he is a consulting scientist to Quality Engineering Associates (QEA), Inc. and others, devoted to understanding the physics and the characterization techniques of electrophotographic materials, processes and devices, in particular, by mathematical analysis. Contact at inanchen@aol.com.